NATIONAL ADVISORY COMMITTEE FOR AERONAUTICS

TECHNICAL NOTE 2381

EFFECT OF HORIZONTAL-TAIL LOCATION ON LOW-SPEED STATIC LONGITUDINAL STABILITY AND DAMPING IN PITCH OF A MODEL HAVING 45° SWEPTBACK WING AND TAIL SURFACES

By Jacob H. Lichtenstein

Langley Aeronautical Laboratory
Langley Field, Va.

Washington

June 1951

NATIONAL ADVISORY COMMITTEE FOR AERONAUTICS

TECHNICAL NOTE 2381

EFFECT OF HORIZONTAL-TAIL LOCATION ON LOW-SPEED STATIC LONGITUDINAL STABILITY AND DAMPING IN PITCH OF A MODEL HAVING 45° SWEPTBACK WING AND TAIL SURFACES

By Jacob H. Lichtenstein

SUMMARY

An investigation has been conducted in the Langley stability tunnel to determine the effects of changes in horizontal-tail location on the static longitudinal stability and on the steady-state rotary damping in pitch of a complete model with wing and tail surfaces having the quarter-chord lines swept back 45°.

The results of the investigation show that, at low angles of attack, although changes in the vertical position of the horizontal tail relative to the wing have significant effects on the static longitudinal stability, these changes have no significant effect on the rotary damping in pitch. The standard methods of calculating the tail contribution to damping in pitch at low angles of attack were found to be reliable for all horizontal-tail locations investigated.

At high angles of attack, the static longitudinal stability characteristics were improved by moving the horizontal tail downward; whereas the rotary damping in pitch generally was increased by moving the horizontal tail upward.

INTRODUCTION

Requirements for satisfactory high-speed performance of aircraft have resulted in configurations that differ in many respects from previous designs. As a result of these changes, the designer has little assurance that the low-speed characteristics will be satisfactory for any specific configuration. The low-speed characteristics of wings suitable for high-speed flight already have been investigated quite

extensively. The contributions of other component parts of aircraft, or of the various combinations of component parts for high-speed airplane configurations, however, are not well understood. In order to provide such information, a series of investigations of models having various interchangeable component parts is being conducted in the Langley stability tunnel. In these investigations the rotary derivatives are being determined by the rolling- and curved-flow techniques (see references 1 and 2) and the static stability characteristics are being determined by conventional wind-tunnel procedures.

The present investigation is concerned with the effect of horizontal-tail location on the static longitudinal stability characteristics and on the steady-state rotary damping in pitch for a swept-wing configuration. The rotary damping in pitch specifies the damping resulting only from curvature of flight path, such as that obtained during a steady pitching maneuver in which the radius of flight-path curvature is constant. For a pitching oscillation, the rotary damping represents only a part of the total damping, since additional contributions may result from unsteady aerodynamic phenomena such as the lag of downwash between the wing and horizontal tail (references 3 and 4).

The model used in the present investigation had 45° sweptback wing and horizontal-tail surfaces with aspect ratios of 4. The model is the same as that used previously in an investigation of the effects of horizontal-tail location on static lateral stability characteristics reported in reference 5.

SYMBOLS

The data presented herein are in the form of standard NACA coefficients of forces and moments which are referred to the stability system of axes, with the origin at the projection on the plane of symmetry of the quarter-chord point of the mean aerodynamic chord of the wing. The positive direction of the forces, moments, angles, and angular velocities are shown in figure 1. The coefficients and symbols are defined as follows:

C_L lift coefficient $\left(\frac{L}{\frac{1}{2}\rho V^2 S_W}\right)$

C_m pitching-moment coefficient $\left(\frac{M}{\frac{1}{2}\rho V^2 S_W \bar{c}_W}\right)$

C_D drag coefficient $\left(\frac{D}{\frac{1}{2}\rho V^2 S_W}\right)$

L lift, pounds

M pitching moment about $\bar{c}_W/4$, foot-pounds

D drag, pounds

ρ mass density, slugs per cubic foot

V velocity, feet per second

S area, square feet

b span, measured perpendicular to fuselage center line, feet

c chord, measured parallel to axis of symmetry, feet

$\bar{c}$ mean aerodynamic chord, feet

l tail length, distance from $\bar{c}_W/4$ to $\bar{c}_H/4$, feet

A aspect ratio $\left(b^2/S\right)$

λ taper ratio, ratio of tip chord to root chord

α angle of attack, measured in plane of symmetry, degrees

ϵ effective downwash angle, degrees

q pitching angular velocity, radians per second

$\frac{qc}{2V}$ pitching-velocity parameter (based on $\bar{c}_W$)

C_{L_α} lift-curve slope, per degree $(\partial C_L/\partial\alpha)$

C_{m_α} pitching-moment-curve slope, per degree $(\partial C_m/\partial\alpha)$

$C_{m_{\dot{\alpha}}} = \frac{\partial C_m}{\partial\left(\frac{\dot{\alpha}c}{2V}\right)}$, where $\dot{\alpha} = \frac{\partial\alpha}{\partial t}$

t time

$C_{m_q} = \frac{\partial C_m}{\partial\left(\frac{qc}{2V}\right)}$

$\left(\Delta C_{m_q}\right)_H$, $\left(\Delta C_{m_\alpha}\right)_H$ increment resulting from addition of horizontal tail (for example, $\left(\Delta C_{m_q}\right)_H = \left(C_{m_q}\right)_{\text{model with H}} - \left(C_{m_q}\right)_{\text{model without H}}$)

Subscripts:

W wing

H horizontal tail

V vertical tail

r radian measure

APPARATUS, MODEL, AND TESTS

The general research model used for the present investigation was designed to permit tests of the wing alone, fuselage alone, or the fuselage in combination with any of several tail configurations - with or without the wing. A sketch of the complete model with one particular tail configuration is shown in figure 2. A list of the pertinent geometric characteristics of various component parts is given in table I. All of the parts were constructed of mahogany.

The fuselage was a body of revolution having a circular-arc profile and a fineness ratio of 6.67. The wing and horizontal tail surfaces had aspect ratios of 4.0, taper ratios of 0.6, and NACA 65A008 airfoil sections parallel to the plane of symmetry; the quarter-chord lines of these surfaces were swept back 45°. Ordinates for the NACA 65A008 airfoil section are given in table II. The vertical tail used had a taper ratio of 0.6, sweep of 45°, and an NACA 65A008 airfoil section, but had an aspect ratio of 1.

The component parts of the general research model were tested in various combinations and, for convenience, each component is identified herein as follows:

Fuselage	F
Wing	W
Horizontal tail	H
Vertical tail	V

The horizontal tail, the incidence of which was kept at 0° for all tests, was tested at three horizontal locations for each of three vertical positions, as illustrated in figure 3. In reference to the horizontal-tail locations, the letters L, C, and U indicate the vertical postion as being lower, center, or upper, respectively; the letters F, M, and R indicate the horizontal location as being forward, middle, or rearward, respectively. A complete list of the configurations investigated is presented in table III.

A photograph of the model with the horizontal tail in the upper rear position is presented in figure 4 to illustrate the test setup in the tunnel. The model was rigidly mounted on a three-support-strut system with the pivot point 4 inches rearward of the quarter-chord point of the mean aerodynamic chord. Forces and moments were measured by means of a conventional six-component balance system.

The tests were made in the 6- by 6-foot test section of the Langley stability tunnel. The dynamic pressure for the tests was 24.9 pounds per square foot, which corresponds to a Mach number of 0.13 and to a Reynolds number, based upon the wing mean aerodynamic chord, of 0.71×10^6. The angle of attack was varied from about -6° to about 32° for the tests. In addition to the straight-flow tests, the tunnel flow was curved to obtain values of $qc/2V$ of 0.008, 0.017, and 0.022. The method of curving the flow consists in curving the tunnel walls to obtain the proper air-stream curvature and inserting, upstream of the test section, screens which give the proper velocity gradient across the test section.

CORRECTIONS

The angle of attack and drag coefficient have been corrected for the effects of jet boundaries. The moment data have been transferred from the mounting point to the quarter-chord point of the mean aerodynamic chord. The damping-in-pitch data have been corrected for the buoyancy caused by the cross-tunnel static-pressure gradient associated with curved flow. The data have not been corrected for blocking, turbulence, or support-strut interference, which are believed to be negligible for the parameters with which this paper is concerned.

RESULTS AND DISCUSSION

Presentation of Results

The basic data obtained in the present investigation are presented in figures 5 to 7. The effects of tail location on the tail contribution to static longitudinal stability and to damping in pitch at zero angle of attack are summarized in figure 8.

The data figures for the various configurations are indexed in table III.

Static Longitudinal Stability

The static-longitudinal-stability parameters obtained from the tests for some basic configurations are presented in figure 5. Inasmuch as these results are very similar to those presented in reference 5 and the analysis of the results are adequately covered in this reference, they are not discussed in this paper.

Data are not presented for the lift and drag of the model with each of the tail arrangements investigated, since the results showed that the lift and drag were negligibly affected by the changes in horizontal-tail location. The lift and drag data presented in figure 5 for the configuration $W + F + V + H_{LM}$ are representative of the lift and drag results for all of the complete model configurations.

The data of figure 7 show that rearward movement of the horizontal tail in either the low, center, or upper positions generally resulted in slightly more negative values of C_{m_α} (increased stability) as would be expected because of the increase in tail length. Raising the horizontal tail also made C_{m_α} more negative in the low angle-of-attack range; however, it made C_{m_α} more positive (decreased stability) in the angle-of-attack range between 10° and 20°. These results are, in general, similar to results of previous investigations of similar nature at both low and high Reynolds numbers (reference 6 and data from the Langley 19-foot pressure tunnel). The increase in stability, at low angles of attack, as the horizontal tail was moved upward was greater than would be expected to result from the increase in tail length which accompanied the upward movement of the tail. Part of this increase in stability, therefore, appears to result from the fact that, in the higher positions, the horizontal tail was above the region of strongest downwash, as is shown in a subsequent section discussing the contribution of the horizontal tail. As the angle of attack increases, however, the horizontal tails mounted in the high positions move into the strong downwash field; whereas the tails in the low position emerge from the downwash field.

From the standpoint of static longitudinal stability, the low horizontal-tail positions appear to be more advantageous than the high tail positions because the change in stability is smallest over the angle-of-attack range for the configurations with the tail in the low positions.

Damping in Pitch

The damping-in-pitch results are presented in figure 6 for the wing-alone and wing-off configurations and in figure 7 for the various complete-model configurations. The value of the damping in pitch for the wing alone is in good agreement with the theoretical value computed by the method presented in reference 7, and the variation with angle of attack is not considered significant. Although a value of C_{m_q} of about -1 was obtained for the fuselage alone (fig. 6), the value of C_{m_q} for the combination of the wing and fuselage was only -2 (fig. 7), which is approximately the same as that for the wing alone. This effect is very similar to that obtained for static longitudinal stability (fig. 5), for which the value of C_{m_α} of the wing-fuselage combination is about equal to C_{m_α} of the wing alone, even though the isolated fuselage has a rather large positive value of C_{m_α}. With the horizontal tail in the low positions, a maximum value of the damping in pitch was obtained at approximately 12° angle of attack (fig. 7(a)); whereas with the tail in the center or upper positions, a maximum was obtained at approximately 20° (figs. 7(b) and 7(c)). The maximum damping would normally be expected to occur at the angle of attack at which the static stability is a maximum (C_{m_α} has its maximum negative value). Comparison of C_m and C_{m_q} curves shows, however, that the opposite occurs (maximum damping occurs approximately where the static stability is a minimum). This apparent incongruity results from the interaction of two opposing effects. The decreased static longitudinal stability occurs when the horizontal tail approaches the wing wake, and the downwash effect becomes greatest when the tail is passing through the wake (approximately 12° angle of attack for the low tails and 20° for the higher tails). There is, however, a favorable variation of downwash with $qc/2V$ because stream curvature displaces the wake upward with respect to the horizontal tail. This favorable effect is greatest when the horizontal tail is immersed in the wake at zero flight-path curvature.

Although the basic data do not show the effect of the vertical position of the horizontal tail clearly, because changes in tail position were accompanied by changes in tail length, the higher horizontal-tail positions appear somewhat more advantageous than the low positions with regard to damping in pitch inasmuch as the variation with angle of

attack was generally smaller and high damping was maintained to nearly maximum lift.

Contributions of the Horizontal Tail

In general, the contributions of a horizontal tail to both static longitudinal stability and to damping in pitch are affected by the downwash from the wing and by the local dynamic pressure in the vicinity of the tail. In the absence of a slipstream and of any important flow separation from the wing, the local dynamic pressure is essentially the same as the free-stream dynamic pressure and the downwash remains as the only factor to be considered. For the present model at low angles of attack, therefore, the tail contribution to static longitudinal stability and to the rotary damping in pitch can be expressed by equations developed by conventional methods of analysis. The tail contribution to static longitudinal stability is given by the following simple relation:

$$\left(\Delta C_{m_\alpha}\right)_H = - \left(C_{L_\alpha}\right)_H \left(1 - \frac{\partial \epsilon}{\partial \alpha}\right) \frac{S_H}{S_W} \frac{l}{\bar{c}_W} \tag{1}$$

An analagous expression can be derived for the tail contribution to the rotary damping in pitch. The pitching moment due to the tail can be written as

$$\left(\Delta C_m\right)_H = - (\Delta\alpha - \epsilon) \left(C_{L_\alpha}\right)_H \frac{S_H}{S_W} \frac{l}{\bar{c}_W} \tag{2}$$

where $\Delta\alpha$ is the change in angle of attack at the tail due to flight-path curvature and is given by

$$\Delta\alpha = 57.3 \frac{l}{\bar{c}_W/2} \frac{qc}{2V}$$

The angle ϵ (measured in degrees) is, in this case, the downwash from the wing or other parts of the airplane and results only from flight-path curvature; that is,

$$\epsilon = 57.3 \frac{qc}{2V} \frac{\partial \epsilon_r}{\partial \frac{qc}{2V}}$$

where ϵ_r, the downwash angle in radian measure, is introduced in order to provide consistent dimensions for both numerator and denominator of the ratio $\frac{\partial \epsilon_r}{\partial \frac{qc}{2V}}$. Substitution in equation (2) of the expressions given for $\Delta\alpha$ and ϵ gives the tail contribution to damping in pitch as:

$$\left(\Delta C_{m_q}\right)_H = -114.6 \left(C_{L_\alpha}\right)_H \left(1 - \frac{\partial \epsilon_r}{\partial \frac{ql}{V}}\right) \frac{S_H}{S_W} \left(\frac{l}{\bar{c}_W}\right)^2 \qquad (3)$$

Equations (1) and (3) indicate that the tail contributions to static longitudinal stability and to damping in pitch are proportional to the geometric quantities $\frac{S_H}{S_W} \frac{l}{\bar{c}_W}$ and $\frac{S_H}{S_W} \left(\frac{l}{\bar{c}_W}\right)^2$, respectively. In the present investigation, however, S_H/S_W was maintained constant at 0.2 and, therefore, $l/\bar{c}_W$ and $\left(l/\bar{c}_W\right)^2$ were the only geometric variables that entered into the equations. The experimental data have, accordingly, been plotted against these quantities in figure 8 for angle of attack equal to zero. The dashed curves on figure 8 were calculated by means of equations (1) and (3) for the values of the downwash parameters $\partial\epsilon/\partial\alpha$ and $\frac{\partial \epsilon_r}{\partial \frac{ql}{V}}$ indicated on the figures. In the calculations, the tail lift-curve slope $\left(C_{L_\alpha}\right)_H$ was assumed to have the same value (0.054) as that of the wing alone (fig. 5), since the wing and tail have the same plan form and section. The fact that the curves for the conditions

$$\frac{\partial \epsilon}{\partial \alpha} = \frac{\partial \epsilon_r}{\partial \frac{ql}{V}} = 0$$

do not pass through the experimental points obtained with the wing removed shows that the fuselage probably had some influence on tail effectiveness.

The data in figure 8(a) indicate that raising the horizontal tail moves it away from the region of strongest downwash since the value of $\partial\epsilon/\partial\alpha$ decreased from about 0.50 to about 0.35 as the horizontal tail was moved from the lower to the upper positions. According to the data

in figure 8(b), however, the value of the downwash parameter $\frac{\partial \epsilon_r}{\partial \frac{q l}{V}}$ which affects the damping in pitch is essentially zero for all tail positions; therefore, the standard methods of calculating the horizontal-tail contribution to C_{m_q} were found to be reliable for all horizontal-tail configurations tested. The positions of the values for the wing-on conditions, relative to the position of the single test value for the wing-off condition indicate, in fact, that the wing contributed a slightly negative value of $\frac{\partial \epsilon_r}{\partial \frac{q l}{V}}$. This result indicates that the wing increases the tail effectiveness for damping in pitch.

A slight increase in tail effectiveness due to the presence of the wing would be expected from consideration of the unusual downwash pattern behind a sweptback wing in pitching flight. For a sweptback wing pitching about the aerodynamic center at zero angle of attack, the center part of the wing, which is forward of the aerodynamic center, is at an effective negative angle of attack and thereby induces an effective upwash at the horizontal tail. The tail, consequently, is at an effective higher angle of attack with the wing on than with the wing off. Since this effect increases with increasing pitching rotation, the wing will tend to increase the damping-in-pitch contribution obtained from the tail at low angles of attack. Some approximate computations were made to determine the upwash at the tail due to pitching flight, and the results indicated the same trend shown experimentally.

Although, at low angles of attack, the vertical position of the horizontal tail was not found to be significant for the steady-state rotary damping in pitch, it might be expected that the vertical position of the horizontal tail would influence the total damping of an airplane in a pitching oscillation. For a pitching oscillation, the total damping is determined by a combination of the rotary derivative C_{m_q}, which has been considered herein, and the acceleration derivative $C_{m_{\dot{\alpha}}}$. The derivative $C_{m_{\dot{\alpha}}}$ is proportional to $d\epsilon/d\alpha$ (see reference 3) and, therfore, should depend rather strongly on the location of the horizontal tail.

CONCLUSIONS

The results of an investigation to determine the effects of horizontal-tail position on the static longitudinal stability and on

the steady-state rotary damping in pitch of a complete model with wing and tail surfaces having the quarter-chord lines swept back 45° indicate the following conclusions:

1. At low angles of attack, although changes in the vertical position of the horizontal tail relative to the wing have significant effects on the static longitudinal stability, these changes have no significant effect on the rotary damping in pitch. The standard methods of calculating the tail contribution to damping in pitch were found to be reliable for all horizontal-tail locations investigated.

2. At high angles of attack, the static longitudinal stability characteristics were improved by moving the horizontal tail downward; whereas the rotary damping in pitch generally was increased by moving the horizontal tail upward.

Langley Aeronautical Laboratory
National Advisory Committee for Aeronautics
Langley Field, Va., February 14, 1951

REFERENCES

1. MacLachlan, Robert, and Letko, William: Correlation of Two Experimental Methods of Determining the Rolling Characteristics of Unswept Wings. NACA TN 1309, 1947.

2. Goodman, Alex, and Brewer, Jack D.: Investigation at Low Speeds of the Effect of Aspect Ratio and Sweep on Static and Yawing Stability Derivatives of Untapered Wings. NACA TN 1669, 1948.

3. Cowley, W. L., and Glauert, H.: The Effect of the Lag of the Downwash on the Longitudinal Stability of an Aeroplane and on the Rotary Derivative M_q. R & M No. 718, British A.R.C., 1921

4. Jones, Robert T., and Fehlner, Leo F.: Transient Effects of the Wing Wake on the Horizontal Tail. NACA TN 771, 1940.

5. Brewer, Jack D., and Lichtenstein, Jacob H.: Effect of Horizontal Tail on Low-Speed Static Lateral Stability Characteristics of a Model Having 45° Sweptback Wing and Tail Surfaces. NACA TN 2010, 1950.

6. Purser, Paul E., Spearman, M. Leroy, and Bates, William R.: Preliminary Investigation at Low Speed of Downwash Characteristics of Small-Scale Sweptback Wings. NACA TN 1378, 1947.

7. Toll, Thomas A., and Queijo, M. J.: Approximate Relations and Charts for Low-Speed Stability Derivatives of Swept Wings. NACA TN 1581, 1948.

TABLE I.- PERTINENT GEOMETRIC CHARACTERISTICS OF THE MODEL

Fuselage:	
Length, in.	40.0
Fineness ratio	6.67
Wing:	
Aspect ratio, A_W	4.0
Taper ratio, λ_W	0.6
Quarter-chord sweep angle, deg	45
Dihedral angle, deg	0
Twist, deg	0
NACA airfoil section	65A008
Area, S_W, sq in.	324
Span, b_W, in.	36
Mean aerodynamic chord, $\bar{c}_W$, in.	9.19
Vertical Tail:	
Aspect ratio, A_V	1.0
Taper ratio, λ_V	0.6
Quarter-chord sweep angle, deg	45
NACA airfoil section	65A008
Area, S_V, sq. in.	48.6
Span, b_V, in.	6.97
Mean aerodynamic chord, $\bar{c}_V$, in.	7.12
Area ratio, S_V/S_W	0.150
Horizontal tail:	
Aspect ratio, A_H	4.0
Taper ratio, λ_H	0.6
Quarter-chord sweep angle, deg	45
Dihedral angle, deg	0
Twist, deg	0
NACA airfoil section	65A008
Area, S_H, sq. in.	64.8
Span, b_H, in.	16.10
Mean aerodynamic chord, $\bar{c}_H$, in.	4.11
Area ratio, S_H/S_W	0.2

Tail-length ratio $l/\bar{c}_W$:

Position of tail	Forward	Middle	Rearward
Upper	2.42	2.58	2.75
Center	2.07	2.24	2.40
Lower	1.66	1.82	1.98

TABLE II.- ORDINATES FOR NACA 65A008 AIRFOIL

[Stations and ordinates in percent airfoil chord]

Station	Ordinate
0	0
.50	.62
.75	.75
1.25	.95
2.50	1.30
5.00	1.75
7.50	2.12
10	2.43
15	2.93
20	3.30
25	3.59
30	3.79
35	3.93
40	4.00
45	3.99
50	3.90
55	3.71
60	3.46
65	3.14
70	2.76
75	2.35
80	1.90
85	1.43
90	.96
95	.49
100	.02
L.E. radius 0.408	

TABLE III.- CONFIGURATIONS INVESTIGATED AND INDEX TO THE FIGURES HAVING DATA ON THESE CONFIGURATIONS

Wing Off		Wing On	
Configuration[1]	Figure	Configuration[1]	Figure
F	5,6	W W + F	5,6
---------- F + V + H_{LM} ----------	6	W + F + V + H_{LF} W + F + V + H_{LM} W + F + V + H_{LR}	5,7(a)
---------- ---------- ----------	--- --- ---	W + F + V + H_{CF} W + F + V + H_{CM} W + F + V + H_{CR}	7(b)
---------- ---------- ----------	--- --- ---	W + F + V + H_{UF} W + F + V + H_{UM} W + F + V + H_{UR}	7(c)

[1]Notation:

W wing
F fuselage
V vertical tail
} For details see figure 2.

H horizontal tail; subscript letters L, C, and U refer to vertical position and letters F, M, and R refer to horizontal location (see fig. 3)

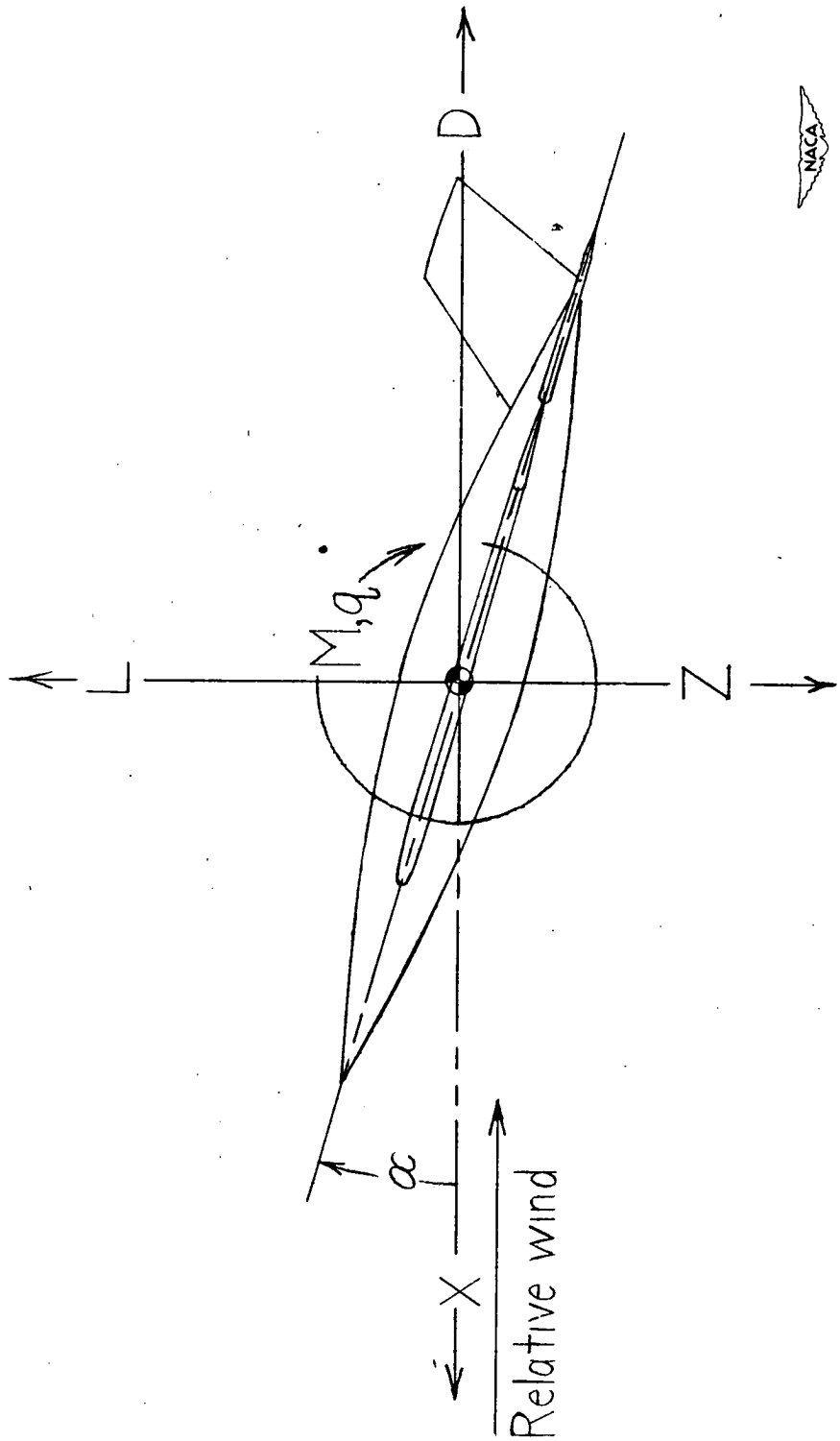

Figure 1.- System of axes used. Arrows indicate positive direction of forces, moments, angles, and angular velocities.

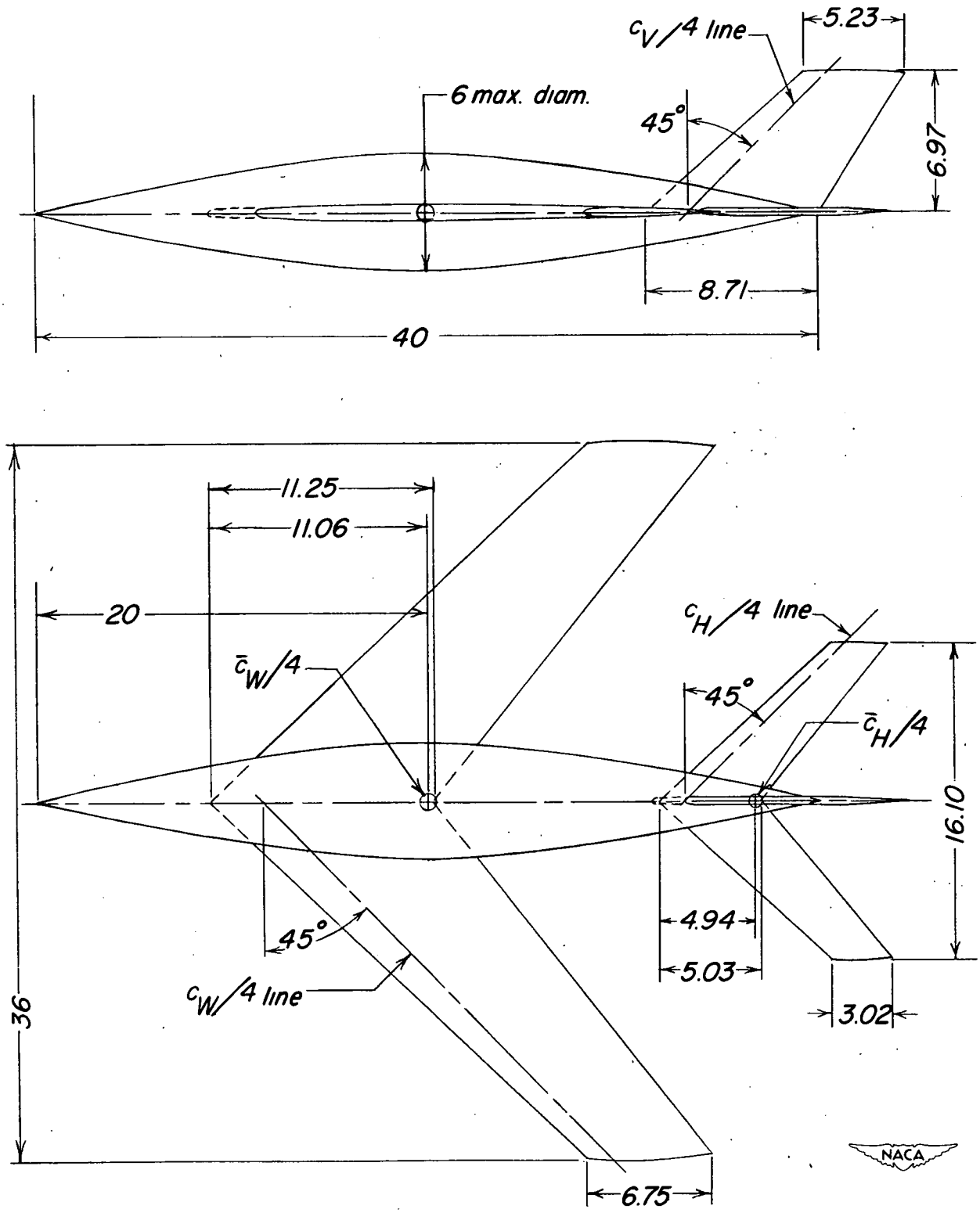

Figure 2.- Dimensions of the complete model. Horizontal tail shown in the lower middle location. (Dimensions are in inches.)

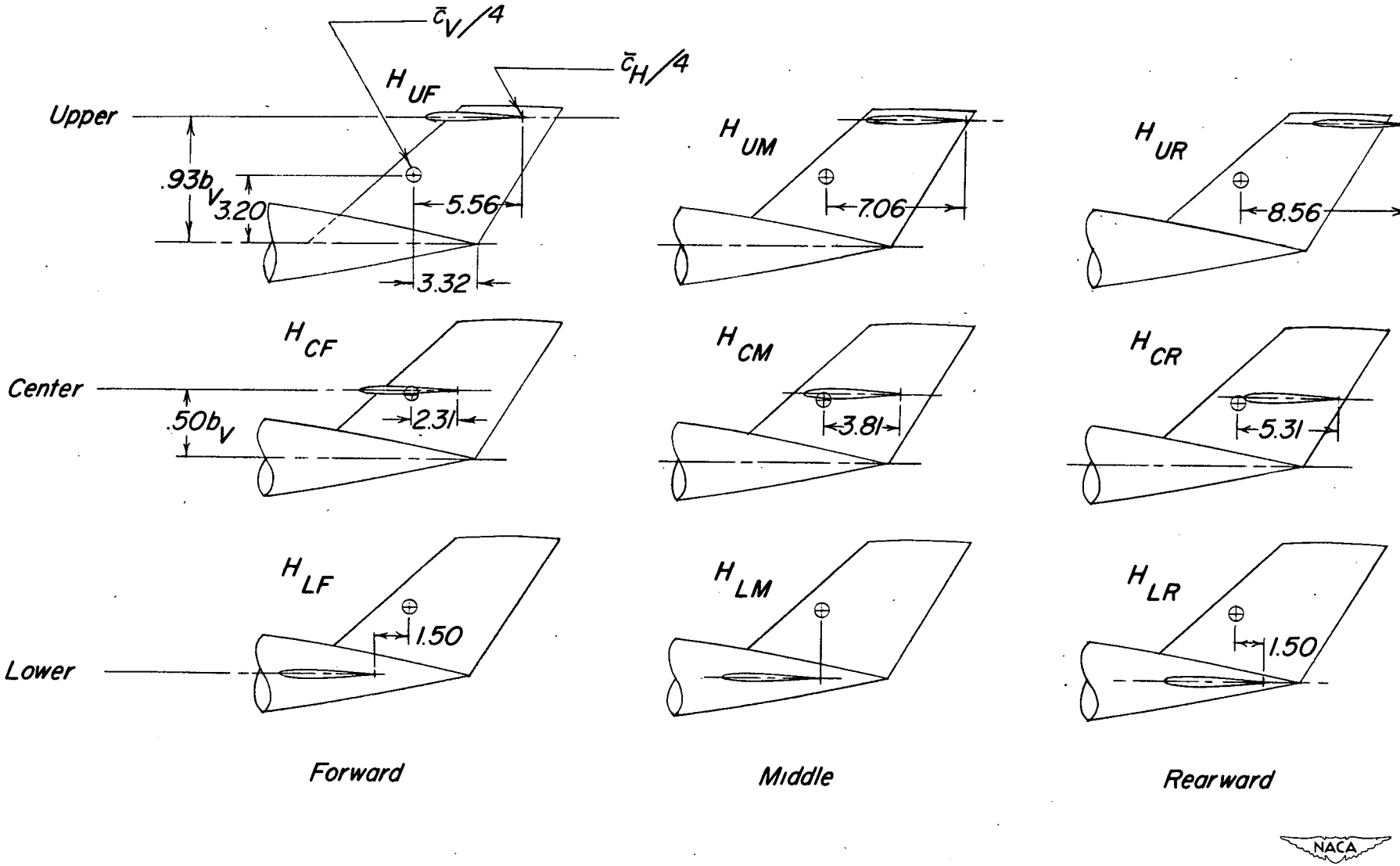

Figure 3.- Location of root chord of horizontal tail for the various configurations. (Dimensions are in inches.)

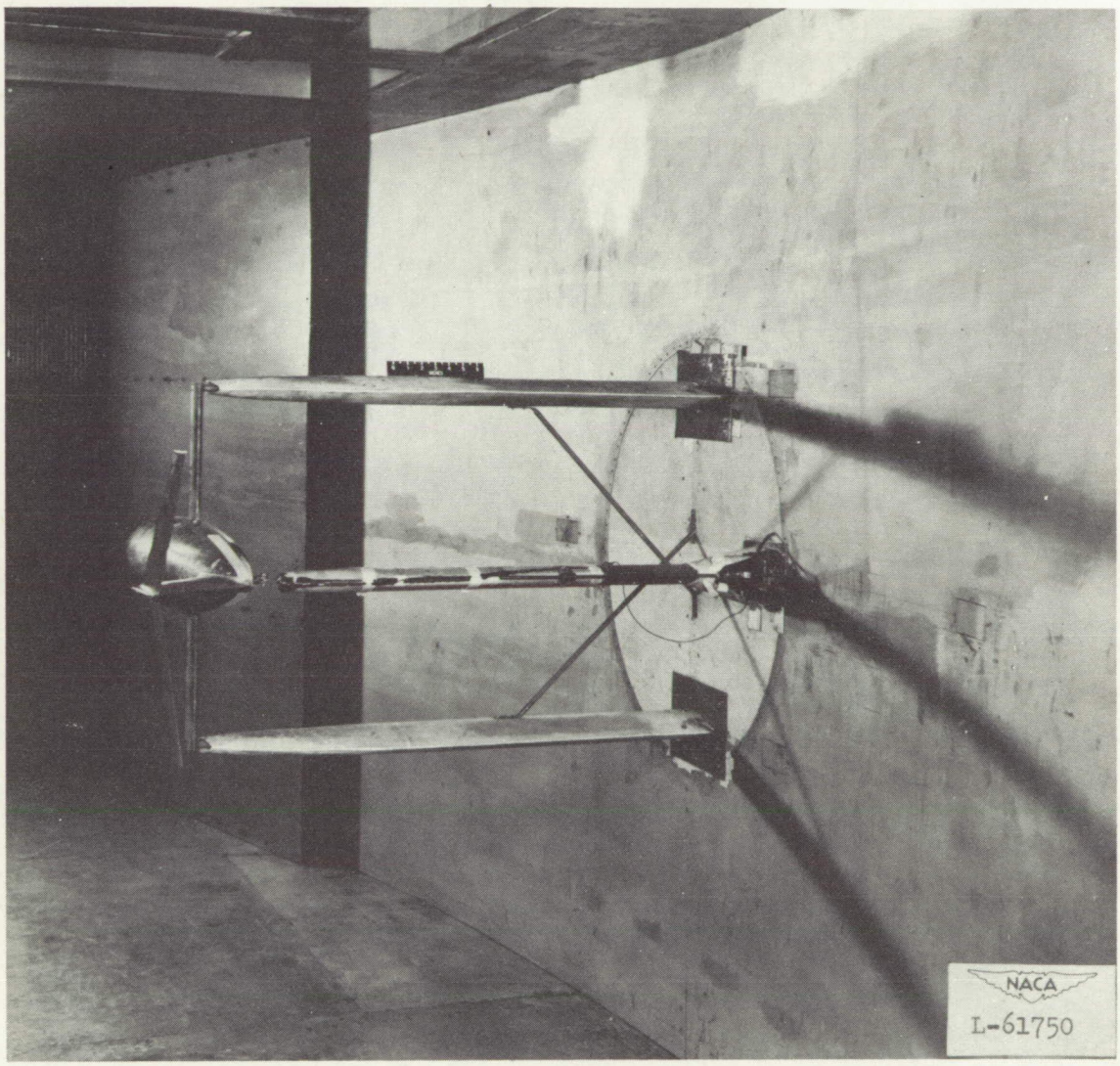

Figure 4.- Model with the horizontal tail in the upper rear location as mounted in the Langley stability tunnel.

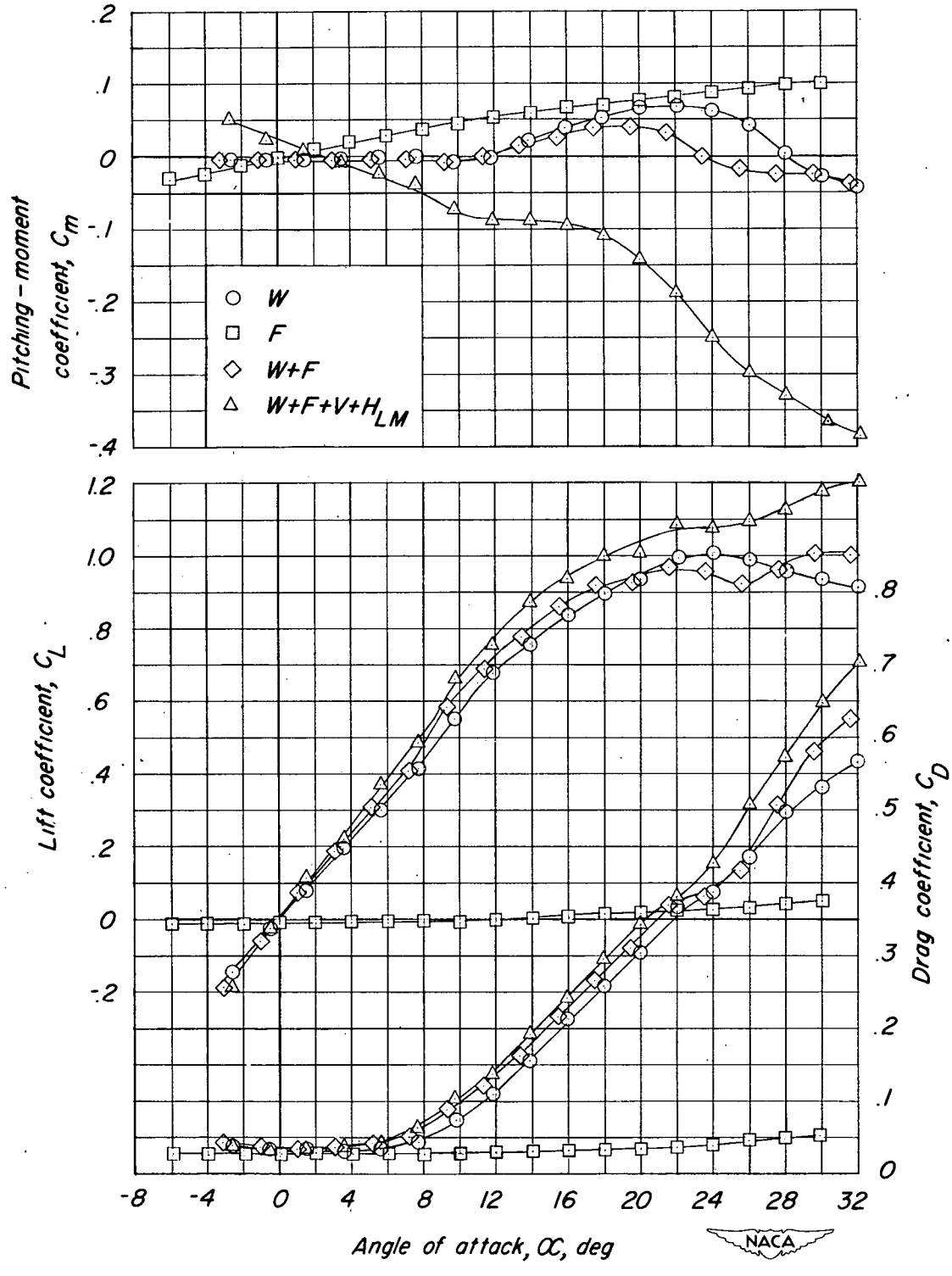

Figure 5.- Aerodynamic characteristics in straight flow of some basic configurations.

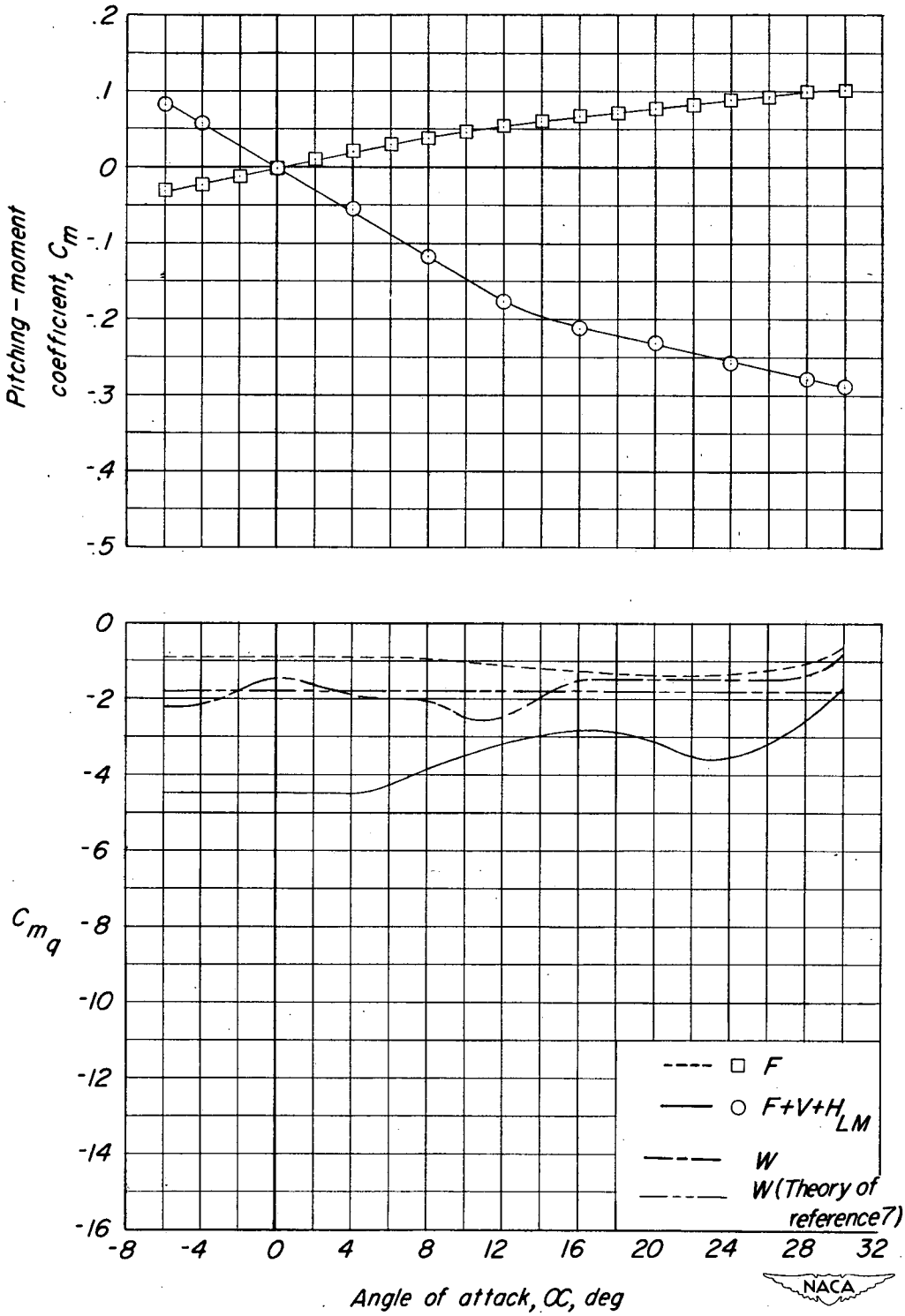

Figure 6.- Variation of static pitching-moment coefficient and damping in pitch of the model with angle of attack. Wing alone and wing-off configurations.

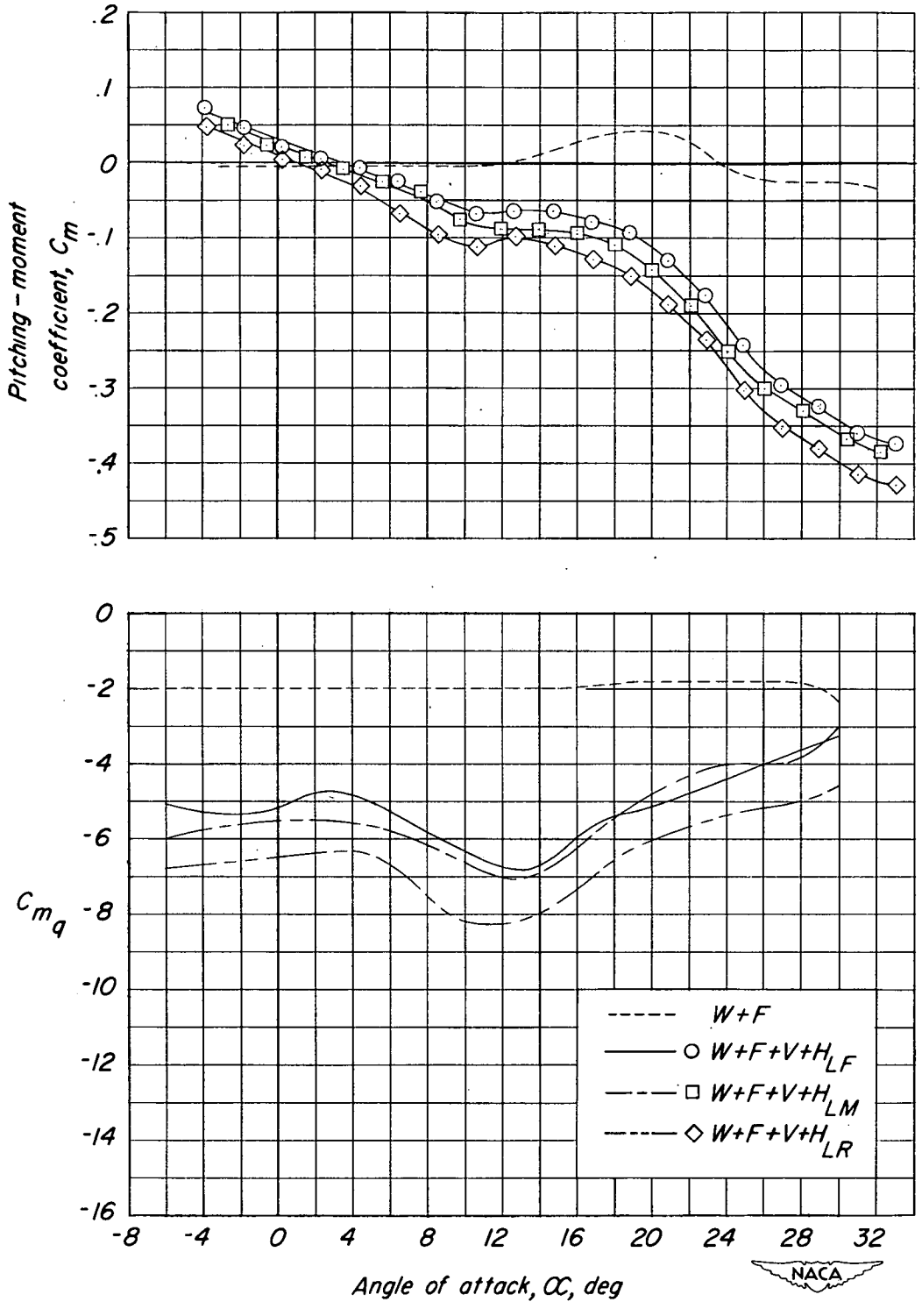

(a) Horizontal tail in low position.

Figure 7.- Variation of static pitching-moment coefficient and damping in pitch with angle of attack. Complete model configurations.

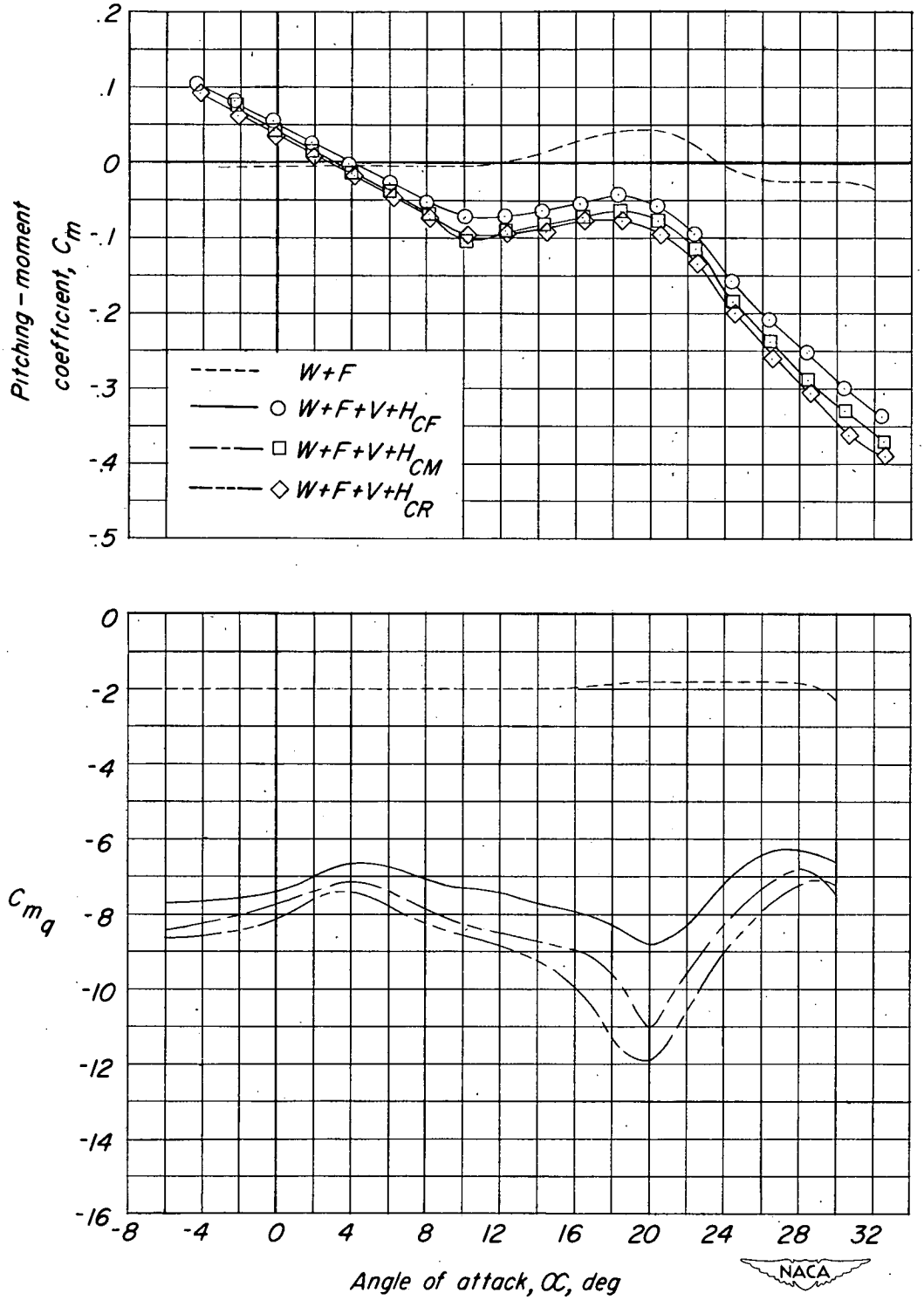

(b) Horizontal tail in center position.

Figure 7.- Continued.

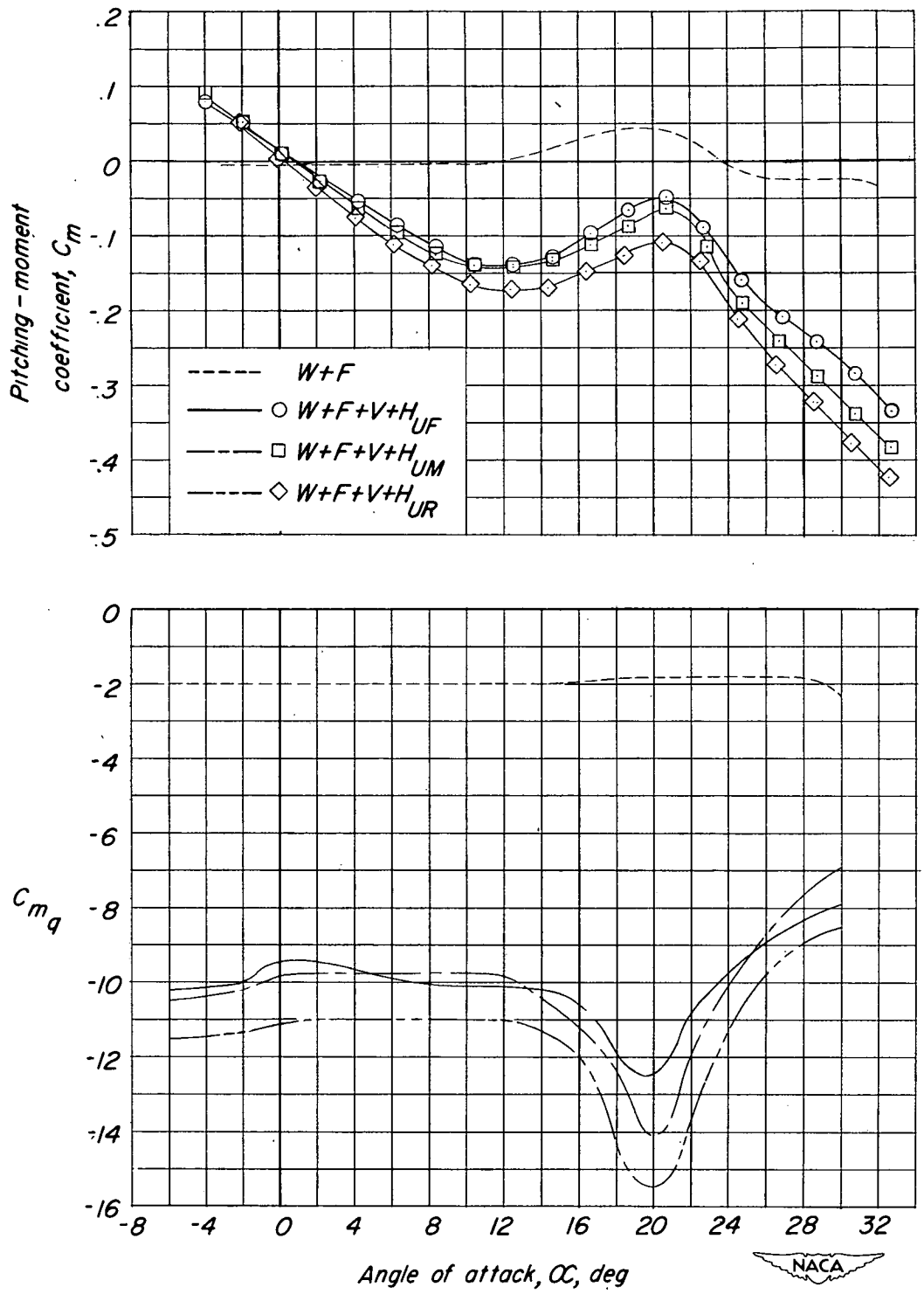

(c) Horizontal tail in upper position.

Figure 7.- Concluded.

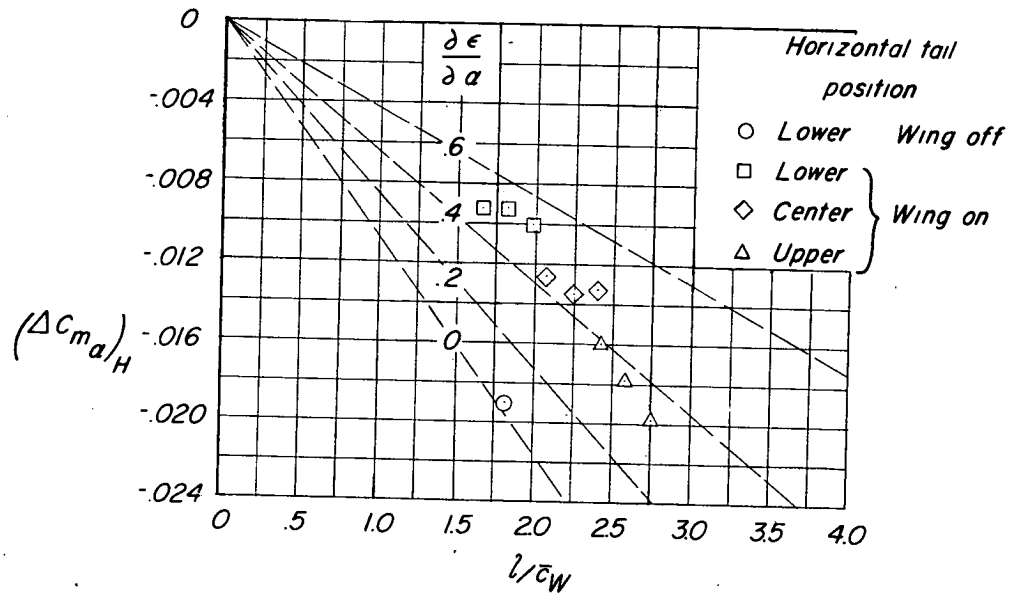

(a) Variation of $(\Delta C_{m_\alpha})_H$ with $\frac{l}{\bar{c}_W}$.

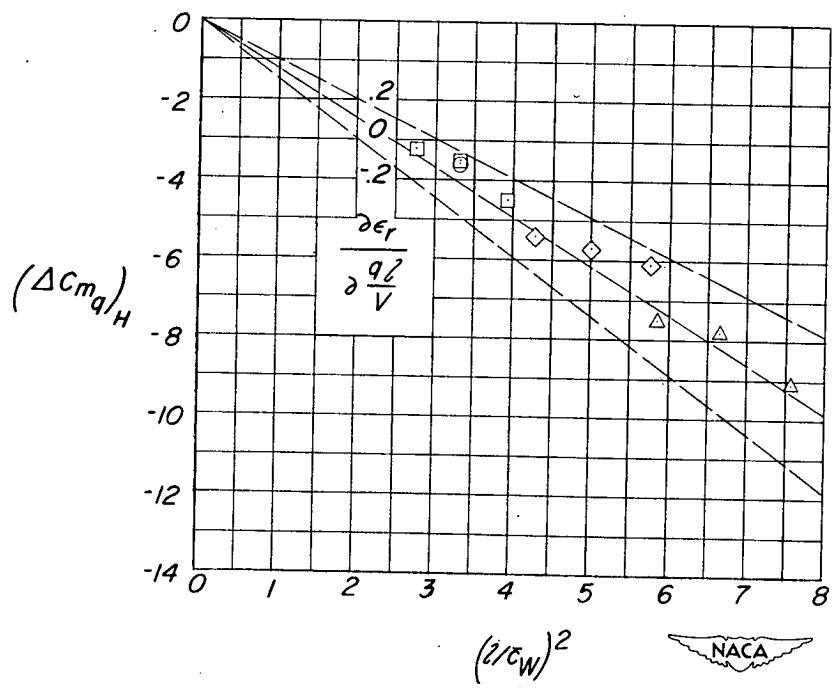

(b) Variation of $(\Delta C_{m_q})_H$ with $\left(\frac{l}{\bar{c}_W}\right)^2$.

Figure 8.- Variation of the increment in static longitudinal stability and damping in pitch due to the horizontal tail with geometric parameters. Lift-curve slope of the horizontal tail was assumed to be 0.54. $\alpha = 0^\circ$.

NACA-Langley - 6-28-51 - 1000

NACA TN 2381

National Advisory Committee for Aeronautics.
EFFECT OF HORIZONTAL-TAIL LOCATION ON LOW-SPEED STATIC LONGITUDINAL STABILITY AND DAMPING IN PITCH OF A MODEL HAVING 45° SWEPTBACK WING AND TAIL SURFACES. Jacob H. Lichtenstein. June 1951. 26p. diagrs., photo., 3 tabs. (NACA TN 2381)

Wind-tunnel results are presented to show the effect of changes in horizontal-tail location on the low-speed static longitudinal stability and steady-state rotary damping in pitch for a complete model with wing and tail surfaces having the quarter-chord lines swept back 45°.

Copies obtainable from NACA, Washington

1. Wings, Complete - Sweep (1.2.2.2.3)
2. Tail-Wing-Fuselage Combinations - Airplanes (1.7.1.1.3)
3. Stability, Longitudinal - Static (1.8.1.1.1)
4. Stability, Longitudinal - Dynamic (1.8.1.2.1)
5. Damping Derivatives - Stability (1.8.1.2.3)

I. Lichtenstein, Jacob H.
II. NACA TN 2381

NACA TN 2381

National Advisory Committee for Aeronautics.
EFFECT OF HORIZONTAL-TAIL LOCATION ON LOW-SPEED STATIC LONGITUDINAL STABILITY AND DAMPING IN PITCH OF A MODEL HAVING 45° SWEPTBACK WING AND TAIL SURFACES. Jacob H. Lichtenstein. June 1951. 26p. diagrs., photo., 3 tabs. (NACA TN 2381)

Wind-tunnel results are presented to show the effect of changes in horizontal-tail location on the low-speed static longitudinal stability and steady-state rotary damping in pitch for a complete model with wing and tail surfaces having the quarter-chord lines swept back 45°.

Copies obtainable from NACA, Washington

1. Wings, Complete - Sweep (1.2.2.2.3)
2. Tail-Wing-Fuselage Combinations - Airplanes (1.7.1.1.3)
3. Stability, Longitudinal - Static (1.8.1.1.1)
4. Stability, Longitudinal - Dynamic (1.8.1.2.1)
5. Damping Derivatives - Stability (1.8.1.2.3)

I. Lichtenstein, Jacob H.
II. NACA TN 2381

NACA TN 2381

National Advisory Committee for Aeronautics.
EFFECT OF HORIZONTAL-TAIL LOCATION ON LOW-SPEED STATIC LONGITUDINAL STABILITY AND DAMPING IN PITCH OF A MODEL HAVING 45° SWEPTBACK WING AND TAIL SURFACES. Jacob H. Lichtenstein. June 1951. 26p. diagrs., photo., 3 tabs. (NACA TN 2381)

Wind-tunnel results are presented to show the effect of changes in horizontal-tail location on the low-speed static longitudinal stability and steady-state rotary damping in pitch for a complete model with wing and tail surfaces having the quarter-chord lines swept back 45°.

Copies obtainable from NACA, Washington

1. Wings, Complete - Sweep (1.2.2.2.3)
2. Tail-Wing-Fuselage Combinations - Airplanes (1.7.1.1.3)
3. Stability, Longitudinal - Static (1.8.1.1.1)
4. Stability, Longitudinal - Dynamic (1.8.1.2.1)
5. Damping Derivatives - Stability (1.8.1.2.3)

I. Lichtenstein, Jacob H.
II. NACA TN 2381

NACA TN 2381

National Advisory Committee for Aeronautics.
EFFECT OF HORIZONTAL-TAIL LOCATION ON LOW-SPEED STATIC LONGITUDINAL STABILITY AND DAMPING IN PITCH OF A MODEL HAVING 45° SWEPTBACK WING AND TAIL SURFACES. Jacob H. Lichtenstein. June 1951. 26p. diagrs., photo., 3 tabs. (NACA TN 2381)

Wind-tunnel results are presented to show the effect of changes in horizontal-tail location on the low-speed static longitudinal stability and steady-state rotary damping in pitch for a complete model with wing and tail surfaces having the quarter-chord lines swept back 45°.

Copies obtainable from NACA, Washington

1. Wings, Complete - Sweep (1.2.2.2.3)
2. Tail-Wing-Fuselage Combinations - Airplanes (1.7.1.1.3)
3. Stability, Longitudinal - Static (1.8.1.1.1)
4. Stability, Longitudinal - Dynamic (1.8.1.2.1)
5. Damping Derivatives - Stability (1.8.1.2.3)

I. Lichtenstein, Jacob H.
II. NACA TN 2381